Supergene gold mineralogy at Ashanti, Ghana: Implications for the supergene behaviour of gold

R. J. BOWELL*

Department of Geology, The University, Southampton SO9 5NH

Abstract

At the Ashanti concession, Ghana, gold-bearing quartz veins and disseminated sulphide lodes occur in narrow (1–3 m) shear zones with altered argillites and metatholeiite host rocks. The mineralisation is concealed by up to 10 m of kaolinite–mica forest ochrosol soils, beneath which is a saprolitic zone of leached rock extending down 60–70 m to the hypogene ore zone. In the unweathered hypogene orebody, gold occurs as free grains in quartz, as sub-microscopic inclusions in the disseminated arsenopyrite, as gold tellurides and as aurostibite. The gold is released from the hypogene orebody by physical dissaggregation and chemical dissolution, the latter involving hydroxyl, thiosulphate, cyanide, and fulvate complexing. Dissolution and reprecipitation of the gold appears to have taken place largely *in situ* with little evidence of supergene enrichment. Consequently, the gold mineralogy of the soils is complex with residual and secondary gold grains exhibiting widely different textural and compositional characteristics. Residually enriched grains display pitted, rounded surfaces and have silver-depleted rims, while supergene gold grains are compositionally homogenous and have unpitted surfaces. The supergene grains display platelet, dendritic, irregular and octahedral habit. A fine grained spongy form of gold has also been observed from weathered telluride-bearing quartz veins. Much of the secondary gold is intergrown with iron oxides and hydroxides. The gold mineralogy of the Ashanti soils appears to be controlled by physico-chemical processes active during the lateritic pedogenesis producing residual and supergene enrichment of gold.

KEYWORDS: gold, supergene mineralisation, Ashanti, Ghana.

Introduction

A tropical rain forest environment is characterised by high rainfall (1250 mm per year), alternating wet and dry seasons and high daily temperatures (20–30 °C) such that chemical weathering occurs at rapid rates. Beneath a deep soil cover lies a saprolitic zone of leached rock extending down to the hypogene ore zone. Weathering of the primary ore zone occurs at the saprolite–rock interface and involves the leaching of mobile components from primary mineral assemblages and the formation of stable secondary assemblages. The saprolite can be sub-divided into lower and upper units with greater oxidation higher in the weathering profile. Continued fluid interaction and leaching of elements results in further loss. This is greatest in the upper portions of the saprolite where the process is further advanced and the textures are more porous. Eventually micro-subsidence occurs, resulting in the loss of the primary fabric marking the soil horizons. The soil profile is composed of a massive clay or B horizon which is separated from the saprolite (or C) horizon by a transitional unit (B/C horizon). Capping the soil profile is the surface or A horizon which is composed of resistant primary minerals, secondary iron oxides/hydroxides and organic matter in a finer argillaceous matrix.

During lateritisation, mineralised shear zones which extend to the surface are also weathered. Alteration zones and intense shearing associated with the mineralisation provide greater fluid access and increase the depth of weathering, resulting in an irregular distribution of weathering fronts around these zones.

At the Ashanti mine, Ghana (Fig. 1), narrow (1–3 m) shear zones contain gold-bearing quartz veins and disseminated sulphides in altered argillites and metatholeiite host rocks. The mineralisa-

* Present address: Department of Mineralogy, The Natural History Museum, Cromwell Road, London SW7 5BD.
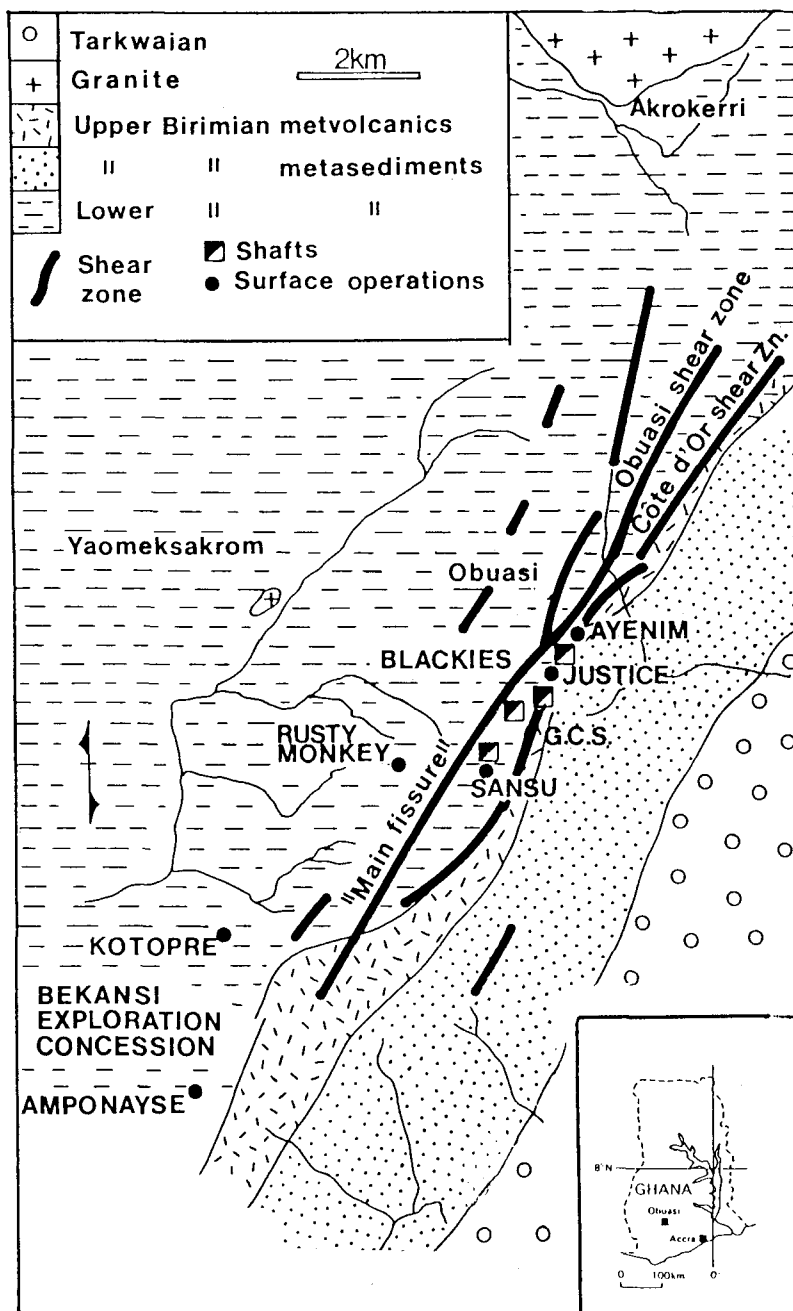
FIG. 1. Location and geology of the Ashanti area (after Amanor, 1979).

tion is concealed by a saprolite zone of leached rock 60–70 m thick and capped by 1–10 m of kaolinite–mica forest ochrosol soils. The gold in the primary mineralisation of the Ashanti mine occurs as (Bowell *et al.*, 1990; Bowell, 1991):

(*i*) free gold in quartz veins and disseminated sulphide lodes;
(*ii*) sub-microscopic or microscopic gold associated with arsenopyrite in disseminated sulphide lodes;

(*iii*) lattice-coordinated gold in arsenopyrite;
(*iv*) gold-bearing minerals in quartz veins, i.e. aurostibite, calaverite, kostovite, petzite and sylvanite.

By discriminant function analysis, the gold-bearing shear zones can be characterised by a multivariant anomaly of Au–Ag–As–Cu–Pb–Zn while the more extensive zones of wallrock alteration are characterised by a Au–As–Cu–Rb–K_2O halo (Bowell, 1991; Bowell *et al.*, 1991). In the soil horizons, gold mineralisation can be delineated by the same multivariant anomalies which closely mimic geochemical dispersion patterns in the bedrock due to the steep angle of dip of the shear zones (65–90°) and the lack of lateral re-distribution of the elements (Bowell *et al.*, 1991).

Gold mineralogy of the saprolite

The supergene behaviour of these three types of primary occurrence, described above, is very different, leading to varying geochemical dispersion patterns of gold in the saprolite, depending on the hypogene mineralogy.

Native gold in the lower saprolite. Gold grains in the lower saprolite vary in size from a few micrometres up to a few millimetres and are similar in composition to the hypogene gold grains. The largest grain found in this study was 5 mm in length, but larger grains have been

recorded (Junner, 1932). The active mining of the past and the present illegal mining have largely removed all the *in situ* gold bearing quartz veins at the surface; this has complicated this study. In the Kotopre prospect (Fig. 1), however, gold-bearing quartz veins are preserved at the surface and here gold occurs along with chalcocite, petzite, scorodite, tellurite, mica and amorphous carbon. Although most of the sulphides and tellurides associated with the gold have been extensively oxidised, gold shows no evidence of oxidation. Gold from the hypogene zone has a composition of 85–91 wt.% Au, 8–15 wt.% Ag (Bowell, 1991) while in the saprolite the composition varies between 87–95 wt.% Au, 5–12 wt.% Ag. Further, the gold grains in the weathered quartz show no chemical or optical zoning as would be expected if preferential loss of silver had occurred (Table 1).

The majority of the gold grains in the weathering profile, particularly those in the saprolite, are rounded with a lobate morphology and the surface is covered by dissolution pits. These grains contain a rim of almost pure gold (average composition 99 wt.% Au, 1 wt.% Ag) and have a core composition similar to the hypogene gold (average 90 wt.% Au, 10 wt.% Ag). Consequently, this gold is considered to represent the remnants of hypogene gold. The gold may be derived from the breakdown of gold-bearing quartz veins and disseminated arsenopyrite lodes within the host rock.

Gold grains in the upper saprolite. The gold

Table 1: Composition ranges of native gold from hypogene and saprolite from drillcore, adits, and trenches, Ashanti, Ghana. All values in weight %

Depth	Au	Ag	Cu
130m	73.76–97.48	2.05–23.3	0.02–0.12
100m	89.27–97.56	2.23–11.1	0.05–0.12
70m	86.56–91.22	8.34–12.0	0.01–0.07
40m	90.43–97.09	1.98–9.21	0.03–0.05
10m	90.67–97.89	2.78–7.34	0.02–0.05
3m	89.67–98.05	1.07–8.56	0.02–0.06
1.9m	90.78–98.08	1.02–7.22	0.02–0.04

All microprobe analysis by Cambridge Instruments Microscan IX. Accelerating voltage of 20kV. Beam current of 2.5×10^{-8}A on the Faraday cage.

Standards: pure elements and PbTe. Radiations measured: Au–Lα, Au–Mα, Ag–Lα, Cu–Kα, Te–Lα, Pb–Mα, Bi–Mα, Pd–Lα

particles present in the upper saprolite show a wide range of textures with most displaying ragged rims with numerous identations (Fig. 2a). Quartz grains, locally associated with a poorly crystalline Fe–Al–Si kaolinite matrix, adhere to the gold particles. Relatively large voids are commonly observed in or between these phases and the gold (Fig. 2a). Most grains, particularly those collected from immediately below the saprolite–soil contact, exhibit dissolution pits ranging from a few micrometres to a few hundred micrometres in size (Fig. 2a). The overall grain size tends to decrease from 50–3000 μm in the lower saprolite to 10–1500 μm in the upper saprolite. The silver content also decreases slightly (Table 1, see analysis for 1.9 m and 3 m), indicating selective dissolution of silver with respect to gold by the supergene fluids.

Within the upper saprolite, chemical weathering of the gold is most active immediately over the mineralised structure, where dissolution pits up to 400 μm in diameter occur. These grains are also more rounded than those at the edge of the gold halo.

The oxidation of arsenopyrite. Arsenopyrite is the most abundant sulphide in the auriferous sulphide lodes and is an important carrier of gold. At the hypogene–lower-saprolite boundary, only slight oxidation occurs with the replacement of arsenopyrite along irregular fractures by scorodite, hematite, bukovskyite, pitticite, kankite, arsenolite and amorphous hydrated ion oxides and arsenates (Fig. 2b). In the lower saprolite, no gold was observed to be associated with the alteration products, nor could any discrete gold phases be observed optically despite gold concentrations (as determined by atomic absorption spectrophotometry) up to 16.6 ppm Au.

In the upper saprolite gold is occasionally visible in polished section in proximity to the pseudomorphed sulphides. The gold occurs as fine (<10 μm) grains up to 300 μm away from the relict arsenopyrite, possibly suggesting some degree of supergene dissolution and re-precipi-
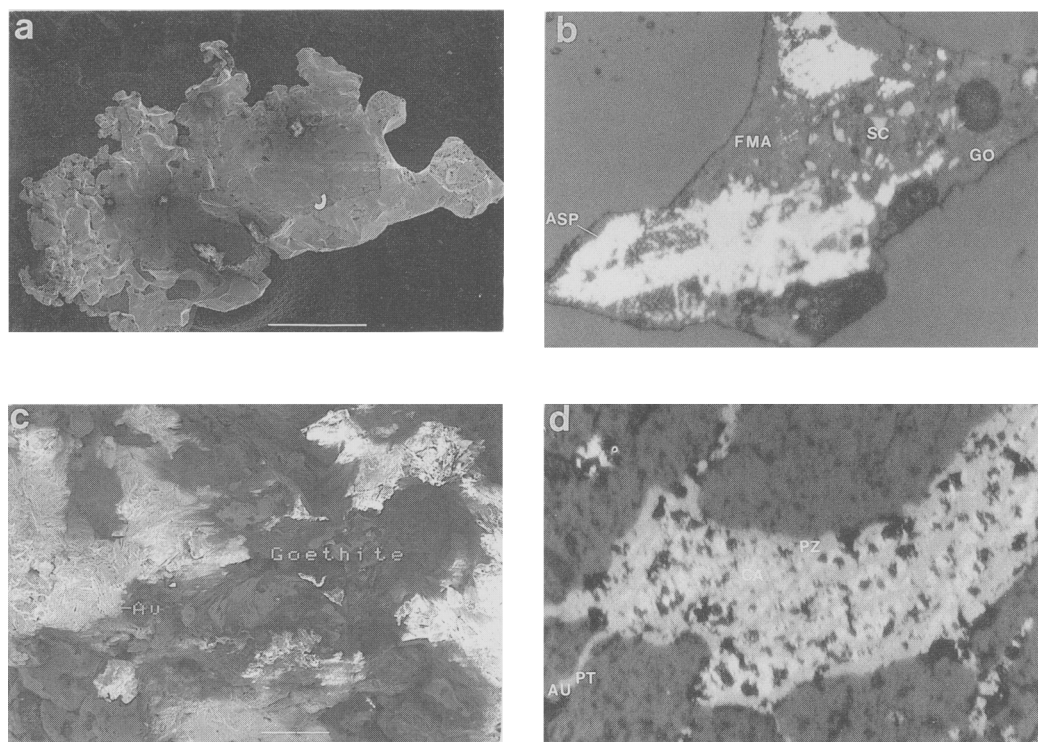
FIG. 2(a–d). (a) Coarse crystalline gold with lobate morphology due to dissolution at the edges ×35. Scale bar 1 mm. Sansu quarry. (b) Relict arsenopyrite (asp) replaced by goethite (go) and scorodite (sc) as well as a range of amorphous Fe–Mn arsenates (FMA) ×10. Field of view, 1 mm. Sansu level 4 main drive. (c) Intergrowth of gold and goethite pseudomorphing arsenopyrite ×70. Scale bar 100 μm. Sansu level 3 adit section. (d) Complex replacement of calaverite (ca) by petzite (pz), paratellurite (pt) and gold (Au) ×20. Field of view, 0.5 mm. Kotopre trench BKT/75.

tation. Disseminations of gold in goethite are common in the highly oxidised orebody (Fig. 2c) and consist of *rusty gold* (Wilson, 1984) an intergrowth of gold and goethite. This supergene mobilisation may be related to complexing by the metastable thiosulphate species.

Occasionally the gold is intermixed with Fe-oxides and hydroxides, producing rusty gold. This is particularly common in the top of the saprolite and at the saprolite–soil interface and is interpreted as the product of the oxidation of gold-bearing arsenopyrite. The arsenopyrite is weathered throughout the saprolite, however, where the arsenopyrite is 'shielded' by quartz grains from the supergene fluids, arsenopyrite grains may persist to the top of the saprolite. Here the arsenopyrite is completely oxidised to goethite, with arsenic either being lost to the supergene fluids or adsorbed by clay minerals. During the breakdown, thiosulphate is produced as an intermediate product in the oxidation of sulphur to sulphate. In the highly oxidising, weakly acidic to neutral environments of the upper saprolite and saprolite–soil interface, the oxidation potential of the environment is sufficiently high to oxidise gold and, where carbonate dissolution buffers pH, gold forms a thiosulphate complex. However, due to the rapid change in the pH of the environment and the greater stability of sulphate over thiosulphate, the complex is unstable and the gold is quickly precipitated out and cements the goethite. The relative stability of the phases produced during the oxidation can be related to the strength of the oxidising supergene fluid and the Eh–pH conditions of the environment in which oxidation takes place. Colloidal reactions may be important in the formation of the secondary arsenates such as scorodite. The iron-manganese precipitates formed, as the initial products of arsenopyrite oxidation, are thermodynamically more stable than scorodite and arsenolite (Boyle and Jonasson, 1973) but are kinetically more unstable (Dove and Rimstidt, 1985). Consequently these amorphous iron–manganese arsenates replace arsenopyrite and are then re-organised to form secondary arsenates:

$$Fe(OH)_3 + H_3AsO_4 = Fe(OH)_3.AsO_4(fixed) + 3H^+$$

$$Fe(OH)_3.AsO_4 + 3H^+ = FeAsO_4.2H_2O- [scorodite] + H_2O$$
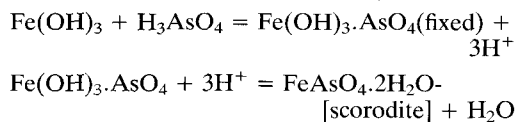
These observations are in agreement with a recent spectroscopic examination of surface alteration during arsenopyrite oxidation (Richardson and Vaughan, 1989).

At a higher level in the saprolite, supergene fluids appear to become more acidic and oxidis-ing. This leads to the de-stabilisation of the arsenates since Fe^{2+} and As_2O_3 are unstable under these Eh-pH conditions. Hematite and limonite replace the secondary arsenate minerals. Arsenic is leached, forming soluble arsenic hydroxides and arsenous acid. Scorodite gradually alters to limonite under intense oxidation, releasing arsenic as arsenous acid:

$$FeAsO_4.2H_2O + H_2O = FeO(OH).H_2O + H_3AsO_4$$
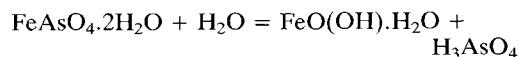
Within the upper saprolite, the remnant sulphides are completely replaced by hematite and limonite (except in some quartz veins). The increase in Eh and decrease in pH in the oxide zone stabilises soluble As species such as arsenous acid leading to the complete loss of arsenates. Hematite and goethite are the stable Fe-species and metastable thiosulphate species may also be produced, although they do alter to the more stable sulphate species with time (Goldhaber, 1983).

The oxidation of gold tellurides and aurostibite. These minerals are rare at Ashanti and not all of them have been observed in the saprolite. The breakdown of gold–silver tellurides in the lower saprolite produces gold, tellurite and an unnamed Au–Ag–Te phase. Within the paratellurite grains, minute grains of gold are present. These are probably a relict of the oxidised tellurides following leaching of silver by groundwaters. In the extensively oxidised samples only paratellurite and gold are present along with cuprite, limonite, lead oxide and quartz. Commonly, fine grained gold and paratellurite (<100 μm) replace petzite and calaverite in complex intergrowths (Fig. 2d).

From the limited data available, Te appears to be relatively immobile in the weathering profile, but hypogene tellurides are altered to supergene tellurides. Consequently, calaverite and sylvanite are replaced first by petzite which in turn is replaced by tellurite and a fine grained (100–700 μm) spongy aggregate of gold termed *mustard gold* by Wilson (1984). The oxidation of tellurides represents a potential source of soluble gold, as a Te-complex, in the supergene fluids (Kelly and Goddard, 1969), although there is no thermodynamic data to support the stability of gold–tellurium complexes in a supergene environment. The greater solubility of Ag compared to Au is observed in the oxidation of the tellurides, with the complete removal of silver from the weathered tellurides and the lower silver content of native mustard gold replacing the hypogene telluride assemblage.

Gold mineralogy of the soil profiles

The gold grains in the soils at Ashanti can be divided into two broad groups; the *residual gold grains*, which are remnant hypogene gold grains and *supergene gold grains* which have formed *in situ*. The compositions of the different morphological groups are given in Table 2 and are shown schematically in Fig. 3. All of the supergene gold grains have similar gold and silver composition variations across the grains despite the different morphologies.

Residual gold grains. The residual gold grains are rounded and heavily pitted due to dissolution of the gold-silver alloy by groundwaters (Figs. 4a–b). These grains are typically 100 μm–2 mm in size although grains up to 5 mm have been observed. Most of the gold grains examined from the saprolite directly over the gold-bearing quartz veins display rounded lobate morphology and are residual hypogene gold grains which decrease in size and frequency upwards and away from the quartz veins. Grains vary from 100 μm to 3 mm and they show a rim (10 to 200 μm thick) of pure gold surrounding a silver rich centre with a core composition similar to the hypogene gold from the quartz vein (90 wt.% Au, 10 wt.% Ag).

In pit 18 of the Amponayse prospect (Fig. 1)

Table 2: Composition range of Soil Gold Grains at Ashanti

Residual Gold Grains, pitted

Morphology	Au (wt.%)	Ag (wt.%)	Cu (wt.%)
round nugget rim	98.0–100.0	0.0–1.50	0.0–0.07
round nugget core	87.92–96.55	4.50–8.88	0.0–0.25
irregular	90.0–100.0	0.0–8.75	0.0–0.30
rounded wire	87.55–100.0	0.0–9.76	0.0–0.42

Supergene Gold Grains, unpitted

Sample	Au (wt.%)	Ag (wt.%)	Cu (wt.%)
octahedra rim	86.0–99.0	0.2–13.0	0.0–0.5
octahedra core	86.0–99.5	0.2–12.8	0.0–0.4
platelet rim	87.35–100.0	0.0–12.8	0.0–0.5
platelet core	87.23–100.0	0.0–12.8	0.0–0.5

Rusty Gold, intergrowth of gold and goethite

irregular grain	95.5–98.4	2.0–5.65	0.0–0.1
platelet	91.0–96.5	3.5–8.9	0.0–0.05
nugget	94.5–97.5	2.0–5.0	0.0–0.05

Mustard Gold, fine grained gold in weathered telluride vein

powder	90.5–99.5	0.0–9.8	0.0–0.05
crystal	91.5–100.0	0.0–8.5	0.0–0.05

All microprobe analysis by Cambridge instruments Microscan IX. Accelerating voltage of 20kV. Beam current of 2.5x10^{-8}A on the Faraday cage.

Standards: pure elements and PbTe. Radiations measured: Au–Lα, Au–Mα, Ag–Lα, Cu–Kα, Te–Lα, Pb–Mα, Bi–Mα, Pd–Lα
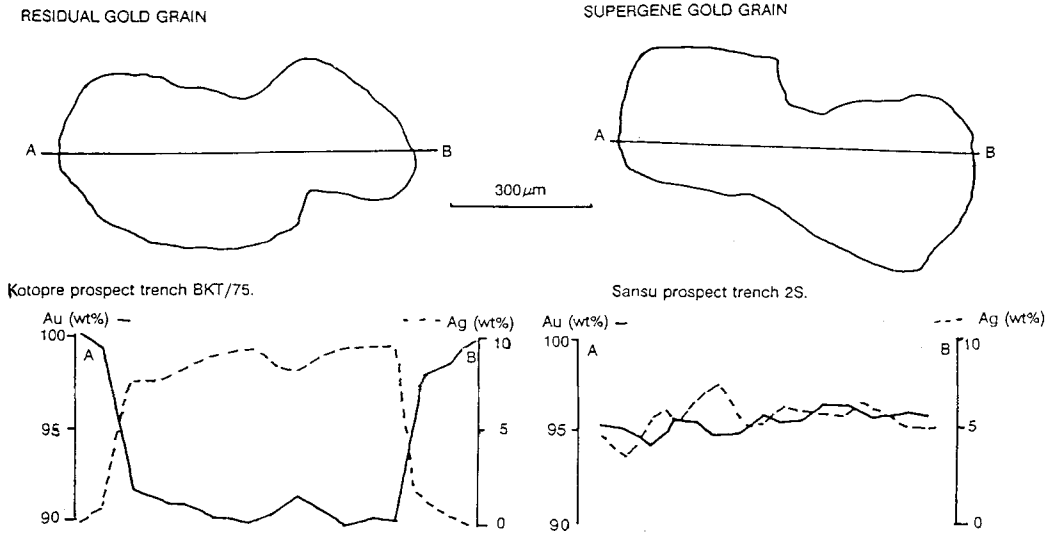
RESIDUAL GOLD GRAIN

SUPERGENE GOLD GRAIN

FIG. 3. Schematic section between soil-gold grains and microprobe traverse across the grains showing variation in gold and silver concentration.

the majority of the gold occurs in soil concentrates directly over the gold-bearing quartz veins. The occurrence of native gold in the quartz vein is reflected in the presence of mainly rounded (residual) hypogene gold grains. In the soil B/C horizon, these grains typically display jagged edges and are coarsely crystalline with a grain size of 300 μm to 4 mm and still adhere to a quartz matrix. Further up the soil profile these grains are heavily pitted and more rounded. Associated with the pitted grains, as elsewhere, are accreted secondary grains which in one case mantle a residual gold grain leading to a zonation of a Ag-rich core (10 to 12 wt.% Ag) coated by a rim (50 μm) of almost pure gold which in turn is coated by secondary gold with 3 wt.% Ag (Fig. 5). Most of the secondary grains displayed a platelet morphology and vary in size from 100 to 500 μm.

From some soil profiles on valley floors, a number of gold grains were collected from the B/C, B and A/B horizons (Fig. 4c). These grains are well rounded and often flat being heavily pitted and scratched (Fig. 4c). The grains vary in size from 500 μm to 5.8 mm, and have a core composition of 95 wt.% Au, 5 wt.% Ag with a rim composition of almost pure gold (99 wt.% Au). These grains appear similar to alluvial gold grains described from elsewhere (Desborough, 1970; Bowles et al., 1984; Bowles, 1988; Groen et al., 1990).

Supergene gold grains. The supergene gold grains form discrete gold crystals, 150–500 μm with octahedral (Fig. 4c), dendritic, wire-like aggregates, and most commonly platelet (Fig. 4d) morphologies. The uncorroded nature of these gold grains and their crystallised forms suggest that precipitation has occurred *in situ* from soil-groundwaters. The homogenous composition of the supergene gold grains (Fig. 3 and Table 2) with no appreciable Ag-depletion or enrichment, has been cited as evidence for supergene gold formation in other localities (Freise, 1931; Fisher, 1935) although this is not always necessary for supergene gold (Wilson, 1984). The gold grains are concentrated in soils directly over the shear zone and the immediate hangingwall. Both the frequency and the size of the gold grains in the soils decreases sharply upwards and away from the shear zone and hangingwall contact. In the B/C horizon, gold–goethite intergrowths occur similar to the *rusty gold* observed in the saprolite (Fig. 2e). This gold shows octahedral and platelet morphologies and has a silver content lower than other forms of supergene gold (Table 2). These grains show very few dissolution pits and consist of roughly equant to elongate platelets which lack any crystallographic faces. They appear to have been formed by the accretion of gold wires and appear to be in a random arrangement and orientation to the platelets making up the grains. The platelets have an average composition of 96 wt.% Au, 4 wt.% Ag. A few grains with heavily pitted platelet morphologies represent secondary gold which has been corroded by the soil waters, since these grains have a core composition of 96 wt.% Au, 4 wt.% Ag, but are mantled by a thin
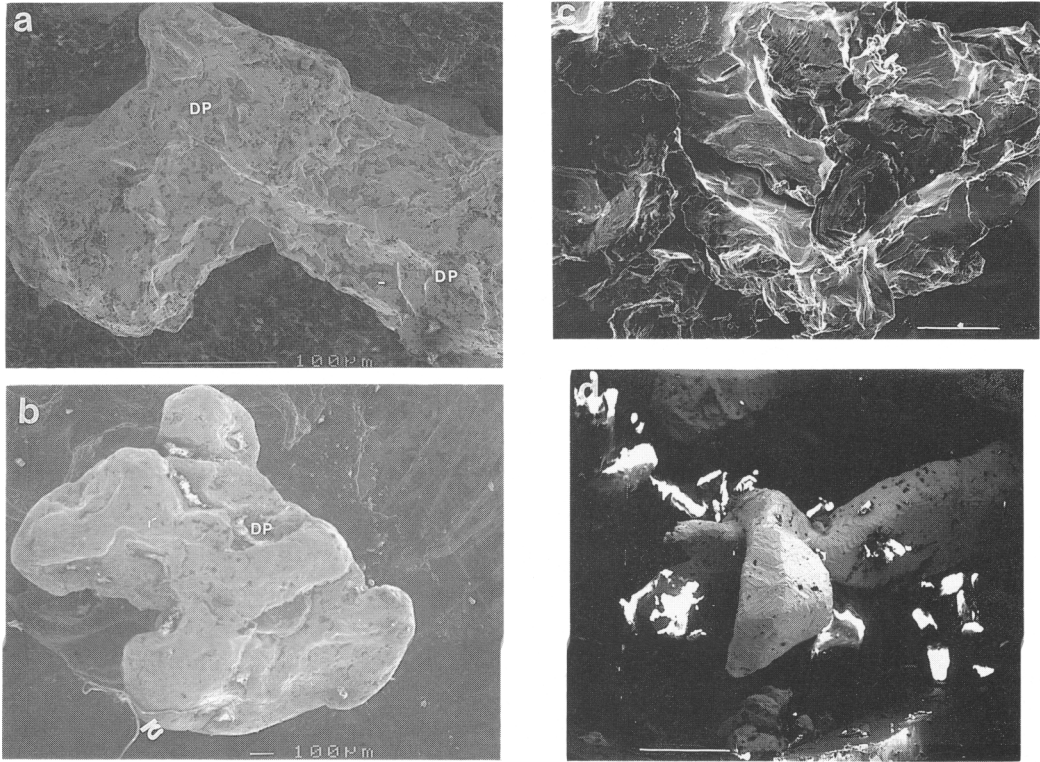
FIG. 4(a–d). (a) Residual gold grain from soils directly over the shear zone. The grain is well rounded and displays a number of dissolution pits due to *in situ* leaching of the gold ×300. Scale bar, 100 μm. Kotopre BKT/75. (b) Residual gold grain showing extensive dissolution of gold ×50. Scale bar, 100 μm. Amponayse line 17 pit 18. (c) Supergene gold grain displaying platelet morphology. Note the lack of dissolution pits ×430. Scale bar, 50 μm. Sansu trench 2S. (d) Octahedral gold developed on wire gold ×60. Scale bar 0.5 mm. Sansu regional traverse site 134.

(10–50 μm) rim of pure gold. The process of precipitation of accreted gold must therefore be due to the re-cycling of gold through numerous cycles of dissolution and precipitation.

In soil concentrates close to the site of a former processing plant in the Sansu prospect (Fig. 1) discrete Au–Hg and Au–Cu–Ag–Hg amalgam grains are present and represent the products of previous mineral processing activities in the area.

Approximately 5% of the gold grains from the saprolite and 40% of the total gold grains extracted from the soil concentrates appear to have formed by *in situ* precipitation from the supergene fluids. These grains exhibit platelet, octahedral, dendritic, and wire-like morphologies and are chemically homogenous (average composition of 96 wt.% Au, 4 wt.% Ag). A similar cementation of soil mineral phases was observed at Kotopre where supergene gold (98 wt.% Au, 2 wt.% Ag) was observed cementing quartz grains

in the soil. Here, some mobilisation of the gold has occurred due to a locally higher pH buffered by calcite dissolution.

The supergene gold grains generally show a homogenous composition and are taken as having formed *in situ*, by precipitation from supergene fluids. The presence of inclusions of Fe-oxides and soil clays such as kaolinite within these grains also supports an *in situ* origin for the gold. The occurrence of supergene gold and of pure gold rims on residual gold grains points to the dissolution of gold within the groundwaters, partial separation of silver from gold and subsequent precipitation of gold. The crystalline nature of the supergene gold, some with unetched crystal faces while others show dissolution pits, suggests these grains are being precipitated by soil waters in the soil and that there is a regular cycle of dissolution and re-precipitation.

Many of the gold grains extracted from the soil horizons were marked by dissolution pits, similar
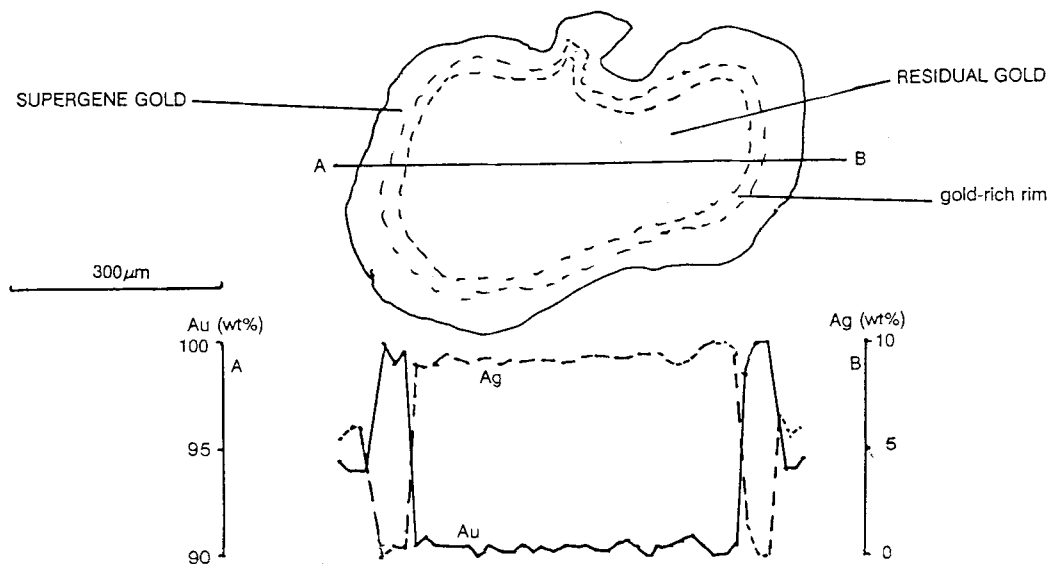
FIG. 5. Schematic section and microprobe traverse across a complex zoned gold grain. Sansu traverse site 134.

to the gold grains extracted from the upper saprolite. These grains show similar rounded lobate textures to the upper saprolite grains and also display gold-rich rims.

Supergene mobilisation of gold in tropical weathering profiles

To explain the observed mineralogical features, a mechanism is required by which both gold and silver can be dissolved, but the consistency in bulk geochemistry, observed throughout the weathering profile at Ashanti (Bowell *et al.*, 1991) must be maintained. Therefore, this precludes extensive migration of the gold.

In the formation of gold-rich rims, there are three mechanisms which will lead to their production (Desborough, 1970; Bowles *et al.*, 1984; Bowles, 1988; Groen *et al.*, 1990); these are:

(*i*) preferential dissolution of silver from the native gold–silver alloy (released from the breakdown of the gold-bearing lodes);

(*ii*) a self-electrorefining process where the Au–Ag alloy at the grain-solution interface dissolves and the gold immediately precipitates back onto the surface of the gold grain;

(*iii*) precipitation of gold onto hypogene native gold–silver alloy from oxidising gold-bearing supergene fluids as it encounters a more reducing environment. The latter mechanism may also be used to explain the formation of the accreted supergene gold grains.

(*i*) *Preferential dissolution of silver.* The most commonly quoted mechanism for the development of gold-rich rims is a process of preferential silver dissolution from the native Au–Ag alloy. Although such a model is chemically reasonable (Desborough, 1970; Mann, 1984; Xue and Osseo-Asare, 1985), it fails to explain how silver atoms from deeper than a few micrometres of the grain can come into contact with the supergene fluid; at Ashanti the gold-rich rims are up to 40 μm thick. Desborough (1970) suggested that the 'oxidation of silver from the metal to the ion reduces its size and affords the needed mobility for removal from its site in the alloy and is thus placed in solution. The porosity resulting from continued silver removal provides a new interface in the gold–silver alloy for a repetition of this process'. But, the sluggish nature of such a reaction (Groen *et al.*, 1990) indicates that such a mechanism is ineffective. In addition, during the commercial refining of electrum, sufficient porosity for selective leaching of silver from electrum is only achieved by 'inquartation' (Bowdish, 1983). In this process the dilution of molten electrum occurs by the addition of two to four times its weight in silver, because the gold in the electrum lattice protects the silver from nitric acid attack. Soil gold grains with a core fineness up to 970 have been observed to develop a distinct rim of 999

fineness (Table 2). Such a small difference in silver content would produce only a small increase in porosity through which supergene fluids are supposed to infiltrate the Au–Ag alloy lattice. Further, those gold grains with a higher silver content in the core (up to 18 wt.%) do not generally develop a thicker Au-rich rim than those with a lower silver content (3–10 wt.%) as would be anticipated if such a mechanism of silver leaching was active (Groen et al., 1990).

Another possible mechanism for silver removal could be the diffusion of silver from the interior of the grain to the surface where it would be dissolved. Groen et al. (1990) calculated the diffusion rates for such a process for placer gold grains and found that to produce a gold rim with a thickness of 8 μm would take 10^{17}–10^{18} years. Furthermore, this mechanism is incapable of yielding the extremely sharp rim–core contacts observed in the grains from the Ashanti soils. Thus, the only conceivable mechanism by which selective silver dissolution could produce a significant gold-rich rim would be by repeated cycles of micron-scale leaching followed by mechanical deformation of the grain exposing a fresh surface of the Au–Ag alloy. The undeformed nature of the residual gold grains in the weathering profile at Ashanti, however, does not support such a mechanism.

(ii) Electrorefining. Electrorefining is a hydrometallurgical process in which a multi-component alloy is electrochemically dissolved, and a generally pure phase of the most inert metal is subsequently precipitated (Fontana, 1986). The driving force of this process is an electrochemical potential difference which can be brought about artificially using a battery or in natural systems as a result of the electrochemical differences between two metals in solution where Eh is higher than that in which the alloy is stable. Since the second mechanism is the more appropriate for natural systems, the process has been termed 'self-electrorefining' (Groen et al., 1990).

Electrochemical experiments show that in a mixed 0.03 M HCl–1M NaCl solution, an increase in Au–Ag alloy stability occurs with increasing gold content, as measured against a pure gold electrode. This demonstrates the lower redox potentials required for dissolution of the silver-rich Au–Ag alloys (Mann, 1984). Once in solution, the less electropositive (and now isolated or 'refined') dissolved gold species accept the free electrons from the gold-rich areas on the hypogene gold surface (Strickland and Lawson, 1973). The gold ions in solution then precipitate back on to the gold grain, effectively forming gold–gold polarisation bonds (Schmidaur et al., 1988). This process also produces the irregular branching dendritic or wire-like textures and lobate gold-rich grain rims observed in the Ashanti gold grains. The more easily oxidised silver is leached by the supergene fluids. The resulting electrolytic reaction is self-perpetuating as a result of the electromotive force (electrical potential difference) between the gold-rich areas and the unrefined native gold–silver alloy.

The process does not require a sharp Eh gradient to precipitate a gold-rich rim, just an ambient solution that is oxidising enough to initiate dissolution of the primary gold. In the presence of ligands such as cyanide, thiosulphate, ammonia and fulvate, this process would be accelerated as redox potentials are lowered.

(iii) Chemical transportation of gold in supergene fluids. At ambient temperatures (25 °C), gold can be complexed by a comprehensive range of ligands and is relatively soluble (Table 3). Depending on the activity of the ligand, the Eh,and pH, several of these ligands are capable of transporting gold in the supergene environment (Lakin et al., 1974; Boyle et al., 1975).

Low-temperature aqueous transportation of gold in the Ashanti soils is indicated by: the presence of measurable quantities of gold in the supergene waters at Ashanti (up to 84.4 μg/l; Bowell, 1991) 40000 times greater than the average gold concentration in natural waters (0.002 μg/l; McHugh, 1988); the gold-rich rims; and the composition and morphology of the secondary gold grains. However, the extent of the gold migration appears to be limited to a metre at the most with negligible lateral or vertical redistribution of gold in the soil profiles at Ashanti (Bowell et al., 1991). Consequently, residual primary grains and accreted secondary gold grains occur together. The preservation of hypogene gold distribution patterns in the weathering profile suggests that the dissolved gold species may migrate over a scale of centimetres before they dissociate.

Since gold is not stable in aqueous solutions as a simple ion, dissolution of the gold must occur by formation of a gold-ligand complex. A number of ligands are capable of complexing gold in sufficient quantity to produce the characteristics of the weathering profile observed. Hydroxyl, halide, thiosulphate, cyanide, and organic complexes are considered to be the most important complexes for supergene gold transport. Thiocyanide complexes will react in a similar way to cyanide and the formation of thiocyanide will depend on the concentration of sulphur in the soils (Seilger, 1981). Ammonia may also form stable gold complexes (Skibsted and Bjerum, 1974) and

Table 3: Chemical reactions of Gold in aqueous solution at 25°C, 1atm.

TRIVALENT GOLD COMPLEXES

Ligand	Reaction	$\Delta G°_f$[1]	$\log \beta$[2]	Ref.[3]
NO LIGANDS				
N.A.[4]	$Au(s) + 0.75O_2 + 3H^+ = Au^{3+} + 1.5H_2O$	433.5	-7.3	F,K
ONE LIGAND				
Cl⁻	$Au(s)+0.75O_2+3H^+ = AuCl^{2+}+1.5H_2O$	239.3	-0.5	B,K
OH⁻	$Au(s)+0.75O_2+2H^+ = AuOH^{2+}+0.5H_2O$	184.9	-9.5	B,K,M
TWO LIGANDS				
Cl⁻	$Au(s)+0.75O_2+3H^++2Cl^- = AuCl_2^++1.5H_2O$	70.7	6.6	B,K
SO₄²⁻	$Au(s)+0.75O_2+3H^++2SO_4^{2-} = Au(SO_4)^-+1.5H_2O$	-1090.4	-7.2	L,K
OH⁻	$Au(s)+0.75O_2+H^++0.5H_2O = Au(OH)_2^+$	-63.6	-7.6	B,K
THREE LIGANDS				
Cl⁻	$Au(s)+0.75O_2+3H^++3Cl^- = Au(Cl)_3+1.5H_2O$	-83.6	11.1	B, K
OH⁻, Cl⁻	$Au(s)+0.75O_2+2H^++2Cl^- = AuOHCl_2+0.5H_2O$	-148.4	3.2	A, K
OH⁻, FA²⁻	$Au(s)+0.75O_2+H^++0.5H_2O+FA^{2-} = Au(OH)_2FA^-$	-----[5]	3.6	J, K
OH⁻, Cl⁻	$Au(s)+0.75O_2+H^++Cl^-+0.5H_2O = Au(OH)_2Cl$	-217.3	-3.7	A,J
OH⁻	$Au(s)+0.75O_2+1.5H_2O = Au(OH)_3$	-283.4	-11.2	K
FOUR LIGANDS				
CN⁻	$Au(s)+0.75O_2+3H^++4CN^- = Au(CN)_4^-+1.5H_2O$	172.4	71.5	E,F,G
NH₃	$Au(s)+0.75O_2+3H^++4NH_3 = Au(NH_3)_4^{3+}+1.5H_2O$	-11.92	51.9	K
I⁻	$Au(s)+0.75O_2+3H^++4I^- = AuI_4^-+1.5H_2O$	-45.0	37.2	K, I
SCN⁻	$Au(s)+0.75O_2+3H^++4SCN^- = Au(SCN)_4^-+1.5H_2O$	561.6	32.1	K
Br⁻	$Au(s)+0.75O_2+3H^++4Br^- = AuBr_4^-+1.5H_2O$	-167.3	21.2	F, K
Cl⁻	$Au(s)+0.75O_2+3H^++4Cl^- = AuCl_4^-+1.5H_2O$	-235.1	14.7	A, K
OH⁻, Cl⁻	$Au(s)+0.75O_2+2H^++3Cl^- = AuOHCl_3^-+0.5H_2O$	-293.6	6.8	A, K
OH⁻, Br⁻	$Au(s)+0.75O_2+H^++0.5H_2O+2Br^- = Au(OH)_2Br_2^-$	-333.7	4.2	F, K
OH⁻, Cl⁻	$Au(s)+0.75O_2+H^+0.5H_2O+2Cl^- = Au(OH)_2Cl_2^-$	-349.7	-3.7	A, K
OH⁻, Cl⁻	$Au(s)+0.75O_2+1.5H_2O+Cl^- = Au(OH)_3Cl^-$	-403.7	-13.4	A, K
OH⁻	$Au(s)+0.75O_2+2.5H_2O = Au(OH)_4^-+H^+$	-455.4	-23.1	A, K
OH⁻, Br⁻	$Au(s)+0.75O_2+1.5H_2O+Br^- = Au(OH)_3Br^-$	-251.9	-35.1	E, K
FIVE LIGANDS				
SCN⁻	$Au(s)+0.75O_2+5SCN^-+3H^+=Au(SCN)_5^-+1.5H_2O$	654.5	31.1	K
OH⁻	$Au(s)+0.75O_2+3.5H_2O=Au(OH)_5^{2-}+2H^+$	-616.5	-36.4	K
SIX LIGANDS				
SCN⁻	$Au(s)+0.75O_2+3H^++6SCN^- = Au(SCN)_6^{3-}+1.5H_2O$	747.0	31.2	K
OH⁻	$Au(s)+0.75O_2+4.5H_2O=Au(OH)_6^{3-}+3H^+$	-763.2	-51.2	K

MONOVALENT GOLD COMPLEXES

Ligand	Reaction	$\Delta G°_f$[1]	β[2]	Ref[3]
NO LIGAND				
N.A.[4]	$Au(s)+0.25O_2+H^+ = Au^++0.5H_2O$	163.6	-28.7	D,K
ONE LIGAND				
S²⁻	$Au(s)+0.25O_2+HS^- = AuS^-+0.5H_2O$	21.6	19.8	E,K,L
HS⁻	$Au(s)+0.25O_2+H^++HS^- = AuHS+0.5H_2O$	35.6	24.5	G,M
SO₃²⁻	$Au(s)+0.25O_2+H^++SO_3^{2-} = AuSO_3^-+0.5H_2O$	-393.3	5.2	B, K,L
S₂O₃²⁻	$Au(s)+0.25O_2+H^++S_2O_3^{2-} = Au(S_2O_3)^-+0.5H_2O$	-418.4	3.3	B, K,L
Cl⁻	$Au(s)+0.25O_2+H^++Cl^- = AuCl+0.5H_2O$	5.0	11.4	B, K
OH⁻	$Au(s)+0.25O_2+H_2O = Au(OH)H_2O$	-345.6	20.11	K, M
TWO LIGANDS				
CN⁻	$Au(s)+0.25O_2+H^++2CN^- = Au(CN)_2^-+0.5H_2O$	285.8	38.7	E, L
HS⁻	$Au(s)+0.25O_2+H^++2HS^- = Au(HS)_2^-+0.5H_2O$	15.7	30.1	G, K
SO₃²⁻	$Au(s)+0.25O_2+H^++2SO_3^{2-} = Au(SO_3)_2^{3-}+0.5H_2O$	-9623.3	21.2	B, K, L
S₂O₃²⁻	$Au(s)+0.25O_2+H^++2S_2O_3^{2-} = Au(S_2O_3)_2^{3-}+0.5H_2O$	-1030.2	26.0	B, K, L
NH₃	$Au(s)+0.25O_2+H^++2NH_3 = Au(NH_3)_2^++0.5H_2O$	1.3	21.0	I, K
I⁻	$Au(s)+0.25O_2+H^++2I^- = AuI_2^-+0.5H_2O$	-47.9	19.0	K
SCN⁻	$Au(s)+0.25O_2+H^++2SCN^- = Au(SCN)_2^-+0.5H_2O$	251.0	16.8	K
Br⁻	$Au(s)+0.25O_2+H^++2Br^- = AuBr_2^-+0.5H_2O$	-115.0	12.4	K
Cl⁻	$Au(s)+0.25O_2+H^++2Cl^- = AuCl_2^-+0.5H_2O$	-151.1	9.2	E, K
OH⁻, Cl⁻	$Au(s)+0.25O_2+Cl^-+0.5H_2O = AuOHCl^-$	-215.2	-6.8	E, F
OH⁻, Br⁻	$Au(s)+0.25O_2+Br^-+0.5H_2O = AuOHBr^-$	-199.9	-4.2	K
OH⁻	$Au(s)+0.25O_2+H^++ =Au(OH)_2^-+H_2O$	-275.4	22.1	K, M
DI-GOLD COMPLEXES				
HS⁻, S²⁻	$2Au(s)+0.5O_2+H^++3HS^- = Au_2(HS)_2S^{2-}+H_2O$	21.0	46.7	E, K, L
S²⁻	$2Au(s)+0.25O_2+H^++2HS^- = Au_2S_2^{2-}+H_2O$	116.8	41.1	A, K, L

[1] Standard state free energy of formation of the gold complex or free ion, given in kJ/mol at 25°C and 1 bar.
[2] Stability constant of the formation of the gold complex at 25°C and 1 bar.
[3] References: A- Baes and Mesmer, 1976; B- Barranova and Ryzenko, 1981; C- Gadet and Pourier, 1970; D- Johnson et al., 1978; E- Pourbaix, 1966; F- Puddephatt, 1978; G- Puddephatt, 1987; H- Renders and Seward, 1989; I- Skibsted and Bjerrum, 1974; J- Varshal et al., 1984; K- Wagman et al., 1982; L- Webster, 1986; M- Vlassopoulos and Wood, 1990.
[4] N.A. = not applicable.
[5] No $\Delta G°_f$ available for Fulvic acid in the literature. See section 7.6.

concentrations in groundwaters can reach 15 mg/l (Feth, 1966).

From the Eh–pH constraints for the Au–H_2O system (Vlassopoulos and Wood, 1990), it is apparent that the aqueous activity of the species $AuOH(H_2O)$ is greater than that of the simple hydrated ion, $Au(H_2O)_2{}^+$, down to a pH well below zero. Within the stability field of water, the solubility of gold as hydroxo complexes (ignoring activity coefficients) may theoretically exceed 1 mg/l or $10^{-5.3}$ M (Vlassopoulos and Wood, 1990). The solubility of this complex is several orders of magnitude higher than the highest value obtained for gold in the natural waters at Ashanti or elsewhere (Brooks et al., 1981; Goldberg, 1987; Koide et al., 1988; McHugh, 1988).

Since low-temperature natural waters are generally not saturated with metallic gold, then calculations of gold solubility in natural waters represent an upper limit which is rarely, if ever, obtained. Consequently, the geochemical cycling of gold, like many trace elements in natural waters, will be a function of gold concentration in the source media and the rate of gold transfer into dissolved forms either as soluble complexes or as colloids. Among these factors, the rate of transfer to solution is of most significance, since the average abundance of gold in crustal rocks is quoted as 4 ppb (Levinson, 1980). This is more than three orders of magnitude higher than the average for natural waters, 0.002 µg/l (McHugh, 1988). Homogenous reactions involving gold in solution will typically attain equilibrium much faster than dissolution reactions, so speciation calculations can be used to determine the most likely forms of gold in the supergene environment. Solubility calculations by Krauskopf (1951), based on the data then available, indicated that $AuCl_4{}^-$ is the dominant species in oxidised, neutral to acidic waters. The limited stability of this species was later confirmed by Cloke and Kelly (1964). In river water, at pH 4, $AuCl_2{}^-$ is considered the main species, whereas, at pH 9, $Au(OH)_4{}^-$ is more stable (Ong and Swanson, 1969). More recently Colin and Viellard (1991) have proposed chlorine as the major ligand for gold migration in the organic-poor regions of the saprolite developed over gold-bearing quartz veins in the tropical environment at Dondo Mobi, Gabon.

Baranova and Rhyzhenko (1981) calculated the solubility of gold in the Au–Cl–S–Na–H_2O system from thermodynamic data. They inferred that gold complexing occurs mostly in neutral to alkali pH waters. The stability of the gold–hydroxo-chloride complex has also been inferred from field observations and thermodynamic calcula-

tions for the Congo watershed by Benedetti and Boulegue (1990). Webster (1986) considered the solubility of gold in the system Au–S–O_2–H_2O as a model system for groundwaters in the environment of oxidising sulphide ores. Her calculations indicated that during the weathering of gold-sulphide ores, thiosulphate and polythionite complexes can account for the supergene migration of gold over the Eh–pH range of natural waters.

In the absence of other ligands, the predominant form of gold (I) will be $Au(OH)(H_2)°$ in the pH range characteristic of natural waters at Ashanti (4–7). However, because natural waters typically contain several potential ligands in variable concentrations, it is important to assess the contribution of the other complexes in natural waters. Among the important inorganic ligands are halides and S-donor species.

The system Au–X–H_2O for X = Cl, Br, I, based on stability constants from Garrels and Christ (1965), Jorgensen and Pouradier (1970) and Vlassopoulos and Wood (1990), shows that the complex $AuOH(H_2O)$ will predominate over AuX^- or $AuXOH^-$ species over the pH and pX^- range typical of the soil waters at Ashanti (Fig. 6). In a similar diagram for thiosulphate (based on stability constants calculated by Webster, 1986) thiosulphate will predominate over the hydroxy complex (Fig. 7). To stabilise gold-thiosulphate complexes, a sulphur activity above 10^{-8} is necessary in acidic and neutral waters, with slightly lower sulphur concentrations required in alkaline waters.

Other inorganic ligands may be of significance in gold complexing. From the stability constants of gold–ammonia calculated by Wagman et al. (1982) it appears that simple hydroxy complexes of gold will predominate over ammonia complexes. Cyanide, produced by the breakdown of peptides and to a lesser extent by the hydrolysis of cyanogenetic glycosides (Conn, 1969; Seilger, 1981) has been proposed as an important ligand for gold mobilisation in soils and natural waters (Lakin et al., 1974; Groen et al., 1990). At Ashanti, gold–cyanide ligands predominate not only over hydroxy complexes but over all other inorganic complexes as well (Fig. 7).

The presence of soluble organic ligands such as fulvic and amino acids will also effect gold solubility (Baker, 1978; Varshal et al., 1984). In the weakly acidic to neutral soils at Ashanti, humic acid is only sparingly soluble in the soil waters. However, fulvic acid is very soluble and therefore will be the dominant dissolved organic species (up to 80%) in the soil waters with minor amounts of amino acids, phenols and sugars (Bowell, 1991). Furthermore, from chemical and
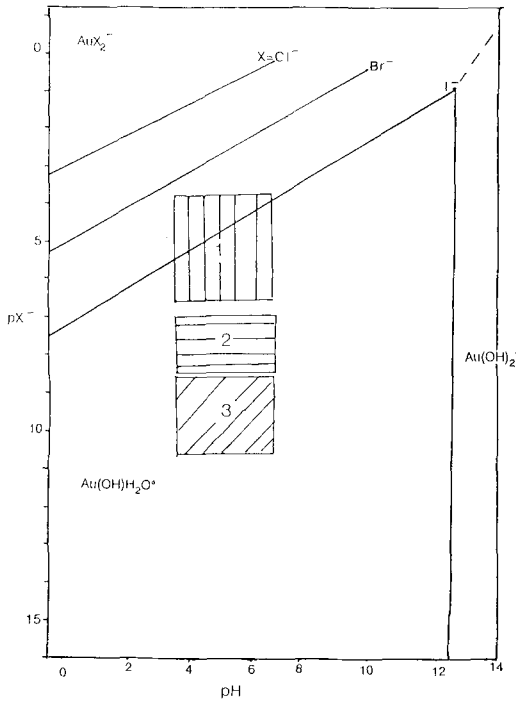
FIG. 6. pX–pH diagram for gold-halide complexes versus stability of the gold-hydroxide complex. The pX fields are shown for: 1, chloride; 2, bromide; 3, iodide. Data are from Baes and Mesmer, 1976; Bowell, 1991; Kronberg et al., 1979; Vlassopoulos and Wood, 1990; Wagman et al., 1982. The large range in the pH field covers uncertainties in the reported activities.
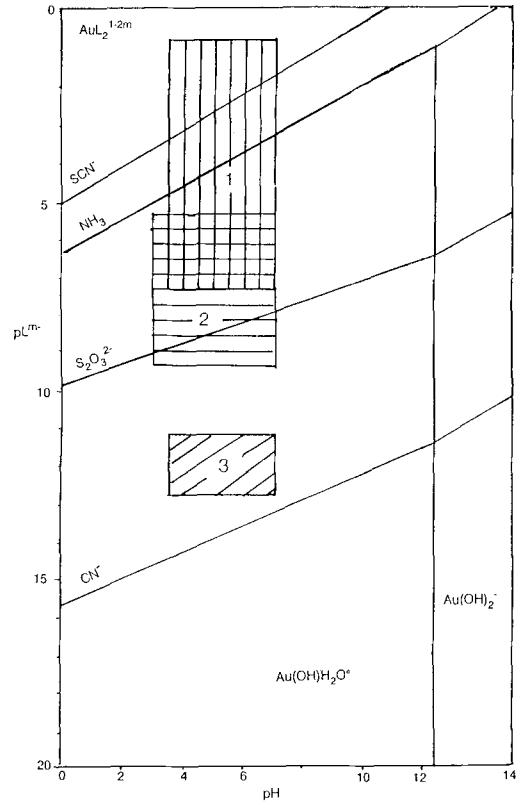

FIG. 7. pX–pH diagram for gold complexes versus the stability of the gold-hydroxide complex. The pX fields are shown for: 1. thiosulphate (Bowell, 1991; Wagman et al., 1982; Webster, 1986). 2. Cyanide (Bowell, 1991). 3. Ammonia (Skibsted and Bjerum, 1974).

structural analysis of the humic substances in the Ashanti soils, fulvic acid contains more O-, N- and S-bearing functional groups than the humic acid and has a lower molecular weight and consequently is chemically more reactive. However, the nature of the gold-bearing species is uncertain. Evidence for the dissolution of gold by humic substances has been presented by Freise (1931), Boyle et al. (1975), Baker (1978), Varshal et al. (1984) and Colin and Viellard (1991).

From the measurement of the reaction of fulvic acid with gold, potassium chloroaurate (III), gold–silver alloy, and calaverite with time, first-order reaction rates were recorded, with gold salts being more soluble than metallic gold (Bowell, 1991). The dissolution of gold by fulvic acid was increased by increasing the concentration of fulvic acid in solution, pH, and the sulphur content of the fulvic acid. From spectroscopic studies of the interaction of different fulvic acids and simple organic acids with gold, the preference for sulphur was shown by the break-

down of mercapta bonds and the formation of C–S bonds after the reaction with gold (Bowell, 1991). High sulphur fulvic acid complexed between 40–50% more gold at any given pH or fulvic acid concentration. The complexes which form between gold and fulvic acid appear, from experimental modelling with simple organic acid ligands (benzoic, benzene-1,2-dicarboxylic, 2-hydroxybenzoic, 2-aminobenzoic, 2-mercapta-benzoic, ethanoic, and ethandioic acids), to have a stoichiometry of AuL_2^{3-} or AuL_2^- or AuL^- (Vlassopoulos et al., 1990; Bowell, 1991), although Varshal et al. (1984) proposed a stoichiometry of $Au(OH)_2FA^-$ from theoretical calculations. The trends in stability of complexes formed between gold and simple organic ligands can be used to draw inferences on the affinity of gold for particular sites within fulvic acid. The general order of stability of gold-organic complexes is S $\gg$ N > O. The gold content of the

Ashanti soil waters ranges from <0.01 µg/l to 84.4 µg/l, whereas disolved organic matter reaches concentrations of 35 mg/l. Since the ratio of gold to organic matter is extremely low, it is likely that all the gold is bonded to sulphur-donor ligands, even though the sulphur content of the fulvic acid is less than 3% (Bowell, 1991).

In the supergene environment, the proportion of fulvic-bound gold complexed by S-functional groups (thiols) will be affected not just by the total concentration of thiol sites, but also by pH, which determines the fraction of the number of available sites for complexing (i.e. the degree of deprotonation). This will be further complicated by competition from other metals such as Cu, Hg, and Ag, which form more stable thiol complexes.

The localised enrichment of gold in tropical soils is not just limited to Ashanti. A similar association of residual and supergene gold grains has been identified in soils overlying a gold-bearing shear zone in the Morobe Goldfields, Papua New Guinea (Webster and Mann, 1984). Here, though, thiosulphate complexing has been used to explain the limited gold dispersion. However, in more equatorial regions, such as the Dondo Mobi goldfields, Gabon (Lecomte and Colin, 1989) or Mborguene goldfields in Cameroun (Freyssinet et al., 1989), gold is widely dispersed in the soils up to 200 mg from the hypogene source. In this environment hydroxy, halide, and organic complexes have been proposed to explain gold mobility (Benedetti and Boulegue, 1990; Colin and Viellard, 1991).

The effects of seasonal variations between wet and dry seasons have yet to be examined in detail; however at Ashanti there is very little difference in groundwater chemistry between wet and dry seasons so the effects would not be great. In other areas, such as the Amazon basin, the extreme variations in water chemistry between wet and dry seasons would have a profound effect on gold mobility as has been shown for other metals (Stallard and Edmond, 1981).

Conclusions

The soil gold mineralogy at Ashanti is the result of lateritic weathering of a gold-bearing shear zone and reflects the hypogene gold mineralogy. The principal form of gold in the hypogene ore is native gold as reflected in the abundance of residual hypogene gold. Active chemical weathering of the shear zones has also produced supergene gold accreted by the dissolution of gold from the alloy as well as liberation from oxidised

arsenopyrite (either as inclusions in arsenopyrite or held in solid solution) and tellurides.

Lack of lateral dispersion of gold in the soils and the restricted endogenic halo suggests a limited migration of the gold-complexes with dissolution and re-precipitation essentially in situ. In this environment complexes with limited stability such as thiosulphate and cyanide can clearly play an active role in gold dissolution.

In the saprolite, the limited gold dissolution is governed largely by the stability of the hydroxide complex, with thiosulphate complexing important where oxidising sulphides are associated with gold. These complexes may also be important in the soils. From this study it appears that gold dissolution and migration in tropical soils at Ashanti are dominated by organically derived ligands such as cyanide, fulvic acid, and amino acids, all of which are the decomposition products of the leaf litter. Halides are not considered important in the soil gold chemistry at Ashanti due to the weakly acidic environment and the low concentration in tropical soils. Likewise humic acids will play a negligible part due to their low solubility in acidic soil waters.

References

Amanor, J. (1979) The geology of Ashanti gold mines and implications for exploration. MSc. thesis (unpubl.), University of London.

Baes, C. F. J. and Mesmer, R. E. (1976) The hydrolysis of cations. J. Wiley and Sons.

Baker, W. E. (1978) The role of humic acids in the transport of gold. Geochim. Cosmochim. Acta., 42, 645–9.

Barranova, N. N. and Rhyzenko, B. N. (1981) Computer simulation of the Au-Cl-S-Na-H_2O systems. Geokhimiya, 18, 989–1001. [in Russian].

Benedetti, M. and Boulegue, J. (1990) Transfer and deposition of gold in the Congo watershed. Earth Planet. Sci. Lett., 100, 108–17.

Bowdish, F. W. (1983) Fire assay for gold and silver. In Proc. Int. Conf. on Gold and Silver (Y. S. Kim, ed.) 7–10. Reno, Nevada.

Bowell, R. J. (1991) The mobility of gold in tropical rain forest soils. Unpubl. PhD thesis. Univ. of Southampton.

——Foster, R. P., and Stanley, C. J. (1990) Precious and base metal telluride mineralisation, Ashanti, Ghana. *Mineral Mag.*, **54**, 617–27.

——————Gize, A. P., Hoppis, H. A., Laffoley, N. A., and Rex, A. J. (1991) The mineralogical and chemical characteristics of tropical rain forest weathering profiles; implications for gold exploration. In *Proc. of Brazil Gold'91: The Economics, Geology, Geochemistry, and Genesis of Gold deposits.* (E. A. Laderia, ed.), 713–9. A. A. Balkema.

Bowles, J. F. W. (1988) Mechanical and chemical modification of alluvial gold. *Aus. I.M.M. Bull. Proc.*, **293**, 9–11.

——Cameron, N. R., Beddoe-Stephens, B., and Young, R. D. (1984) Alluvial gold, platinum, osmium-iridium, copper-zinc and copper-tin alloys from Sumatra-their composition and genesis. *Trans. Inst. Min. Metall. (Sect. B)*, **93**, 823–30.

Boyle, R. W. and Jonasson, I. R. (1973) The geochemistry of arsenic and it's use as an indicator in geochemical prospecting. *J. Geochem. Explor.*, **2**, 251–96.

——Alexander, W. M., and Ashin, G. E. M. (1975) Some observations on the solubility of gold. *Geol. Surv. Canada*, **75–24**, 8 p.

Brooks, R. B., Chatterjee, A. K., and Ryan, D. E. (1981) Determination of gold at the ppt level in natural waters. *Chem. Geol.*, **33**, 163–9.

Cloke, P. L. and Kelly, W. C. (1964) Solubility of gold under inorganic supergene conditions. *Econ. Geol.*, **59**, 259–70.

Colin, F. and Viellard, P. (1991) Behaviour of gold in lateritic equatorial environment: weathering and surface dispersion of residual gold particles, at Dondo Mobi, Gabon. *Appl. Geochem.*, **6**, 279–90.

Conn, E. E. (1969) Cyanogenic glycosides. *Agr. and Food Chemistry*, **17**, 838–43.

Desborough, G. A. (1970) Silver depletion indicated by microanalysis of gold from placer occurrences, western United States. *Econ. Geol.*, **65**, 304–11.

Dove, P. M. and Rimstidt, J. D. (1985) The solubility of scorodite $FeAsO_4.2H_2O$. *Am. Mineral.*, **70**, 838–44.

Feth, J. H. (1966) Nitrogen compounds in natural water-a review. *Water Resources Res.*, **2**, 41–58.

Fontana, M. G. (1986) *Corrosion Engineering.* (Third Edition). McGraw-Hill, New York, 353 p.

Freise, F. W. (1931) The transportation of gold by organic underground solutions. *Econ. Geol.*, **26**, 421–31.

Freyssinet, P., Zeegers, H., and Tardy, Y. (1987) Nèofornation de l'or dans les cuirasses latèritiques: dissolution et prècipitation. *C.R. Acad. Sci. Paris*, **305**, Sèrie II, 867–74.

Gadet, M. and Pouradier, J. (1972) Hydrolyse des complexes de l'or (I). **275**, 1061–4.

Garrels, R. M. and Christ, C. L. (1965) *Solutions, Minerals and Equilibria.* Harper and Row, 450 p.

Goldberg, E. D. (1987) Comparative chemistry of platinium and other heavy metals in the marine environment. *Pure Appl. Chem.*, **59**, 576–91.

Groen, J. C., Craig, J. R., and Rinstidt, J. D. (1990) Gold-rich rim formation on electrum grains in placers. *Can. Mineral.*, **28**, 207–28.

Johnson, P. R., Pratt, J. M., and Tilley, R. I. (1978) Experimental determination of the standard redox potentials of gold (I) ion. *J. Chem. Soc. Chem. Comm.*, 1978, 606–7.

Jorgensen, C. K. and Pouradier, J. (1970) Un noveau type de stabilisation des 'champides ligands' dans les complexes linèaines du cuivre (I), de l'argent (I) et de l'or (I). *J. Chem. Phys.*, **67**, 124–7.

Junner, N. R. (1932) *The geology of the Obuasi goldfield.* Memoir Gold Coast Geological Survey, 2, 65 p.

Kelly, W. C. and Goddard, E. N. (1969) Telluride ores of Boulder County, Colorado. *Geol. Soc. Amer. Mem.*, **109**, 237 p.

Koide, M., Hodge, V., Goldberg, E. D., and Bertine, K. (1988) Gold in seawater: a conservative view. *Appl. Geochem.*, **3**, 237–42.

Krauskopf, K. B. (1951) The solubility of gold. *Econ. Geol.*, **46**, 858–70.

Kronberg, B. I., Fyfe, W. S., Leonardos, O. H., and Satos, A. M. (1979) The chemistry of some Brazilian soils: element mobility during intense weathering. *Chem. Geol.*, **24**, 211–29.

Lakin, H., Curtin, G., and Hubert, A. (1974) *Geochemistry of gold in the weathering cycle.* U.S.G.S. Bull. **1330**, 80 p.

Lecomte, P. and Colin, F. (1989) Gold dispersion in a tropical rain forest weathering profile at Dondo Mobi, Gabon. *J. Geochem. Explor.*, **34**, 285–301.

Levinson, A. A. (1980) *Introduction to Exploration Geochemistry.* (2nd Ed.). Applied Publishing.

Mann, A. W. (1984) Mobility of gold and silver in lateritic weathering profiles: some observations from Western Australia. *Econ. Geol.*, **79**, 38–49.

McHugh, J. B. (1988) Concentration of gold in natural waters. *J. Geochem. Explor.*, **30**, 85–94.

Ong, H. L. and Swanson, V. E. (1969) Natural organic acids in the transportation, deposition, and concentration of gold. *Quart. Colo. School. Mines*, **64**, 395–425.

Pouribaix, M. (1966) *Atlas of electrothermal equilibria.* Pergamon Press, Oxford. 645 p.

Puddephatt, R. J. (1978) *The Chemistry of Gold.* Elsevier, Amsterdam. 490 p.

——(1987) Gold. In *Comprehensive Coordination Chemistry—the synthesis, reactions, properties, and application of coordination compounds* (G. Wilkenson, R. Gillard, and J. McCreverly). **5**, Pergamon Press. 869–923.

Renders, P. J. and Seward, T. M. (1989) The stability of hydrosulphido- and sulphido-complexes of Au(I) and Ag(I) at 25 °C. *Geochim. Cosmochim. Acta*, **53**, 245–53.

Richardson, S. and Vaughan, D. J. (1989) Surface alteration of arsenopyrite. *Mineral. Mag.*, **53**, 201–12.

Schmidaur, H., Graf, W., and Müller, G. (1988) Weak intramolecular bonding relationships: The confirmation of attractive interaction between gold (I) centres. *Angew. Chem. Inst. Ed. Engel.*, **27**, 417–9.

Seilger, D. S. (1981) Cyanogenetic glycosides and lipids: structural types and distribution. In *Cyanide in Biology*, 233–67.

Skibsted, L. H. and Bjerum, J. (1974) Studies on gold

complexes II. The equilibrium between gold (I) and gold (III) in ammonia system and the standard potentials of the couples involving gold, diaminegold (I), and tetraaminegold (III). *Acta Chem. Scand.*, **A28**, 764–70.

Stallard, R. F. and Edmond, J. M. (1981) Geochemistry of the Amazon: 1. Precipitation chemistry and the marine contribution to the dissolved load at the time of peak discharge. *J. Geophys. Res.*, **86**, 9844–58.

Strickland, P. H. and Lawson, F. (1973) The measurement and interpretation of cementation rate data. In *Int. Symp. Hydrometallurgy* (D. J. I. Evans and R. S. Shoemaker, eds.). Am. Inst. Min. Metall. and Petroleum Engineers, Inc., New York.

Varshal, G. M., Velyukhanova, T. K., and Baranova, N. N. (1984) The geochemical role of gold (III) fulvate complexes. *Geochem. Int.*, **21**, 139–46.

Vlassopoulos, D. and Wood, S. A. (1990) Gold speciation in natural waters: I solubility and hydrolysis of gold in aqueous solution. *Geochim. Cosmochim. Acta,* **54**, 3–12.

Wagman, D. D., Evans, H. H., Parker, V. B., Schumm, R. H., Harlow, I., Bailey, S. M., Churney, K. L., and Butall, R. L. (1982) The NBS tables of chemical thermodynamic properties. Selected values for inorganic and organic substances in SI units. *J. Phys. Chem. Ref. Data II, supp.* **2: 392**.

Webster, J. G. (1986) The solubility of Au and Ag in the system $Au–Ag–S–O_2–H_2O$ at 25 °C and 1 atm. *Geochim. Cosmochim. Acta,* **50**, 1837–45.

—— and Mann, A. W. (1984) The influence of climate, geomorphology, and primary geology on the supergene migration of gold and silver. *J. Geochem. Explor.,* **22**, 21–42.

Wilson, A. F. (1984) Origin of quartz-free gold nuggets and supergene gold found in soils and laterites—a review and some new observations. *Austral. J. Earth Sci.,* **31**, 303–16.

Xue, T. and Osseo-Asare, K. (1985) Heterogeneous equilibria in the $Au–Ag–CN–H_2O$ system. *Metal. Trans.,* **16B**, 455–63.